

## Supporting Information

*for*

### **Highly Sensitive and Selective Detection of DCP Vapors Using Pyridine-Based Fluorescent Nanofilms**

Zebiao Qiu, Yue Xiao, Ling Zhang, Yupei Miao, Bei Zhang, Xiaolin Zhu,\* Liping Ding,\* Haonan Peng,\* and Yu Fang

Key Laboratory of Applied Surface and Colloid Chemistry (Ministry of Education),  
School of Chemistry and Chemical Engineering, Shaanxi Normal University, Xi'an  
710062, P. R. China

\*Corresponding emails: [phn@snnu.edu.cn](mailto:phn@snnu.edu.cn); [xiaolinchem@snnu.edu.cn](mailto:xiaolinchem@snnu.edu.cn);  
[dinglp33@snnu.edu.cn](mailto:dinglp33@snnu.edu.cn)

## 1. Experimental Details

### 1.1 Materials.

4,4',4'',4'''-(Ethene-1,1,2,2-tetrayl) tetraaniline (97%) was purchased from Bide, 1,4-dibromobenzene ( $\geq 98\%$ ), 4-aminophenylboronic acid pinacol ester (98%), 4,4''-p-terphenyldicarboxaldehyde (97%), tetrakis(triphenylphosphine)palladium (99%, Pd:  $\geq 9.2\%$ ) were products of Adamas. All the solvents used in the study were purchased from China National Medicines Corporation Ltd.

### 1.2 Material Characterization.

The synthesized compounds were characterized by  $^1\text{H}$  NMR (AVANCE III 600, Bruker) and HRMS (Maxis Ultimate 300 HPLC, Bruker). The nanofilms were prepared in a constant temperature and humidity chamber (HWS-70B, FAITHFUL). The chemical composition of the nanofilms was characterized using Fourier transform infrared spectroscopy (SENSOR27, Bruker) and X-ray photoelectron spectroscopy (XPS, AXIS ULTRA). UV-Vis absorption spectra of the nanofilms were collected with a U-3900 spectrophotometer (Hitachi), and fluorescence steady-state emission spectra were recorded using an Edinburgh FLS 980 fluorescence spectrometer. The morphology of the nanofilms was characterized by scanning electron microscopy (SEM, SU8220) and high-resolution transmission electron microscopy (HR-TEM, JEM-2100). The thickness of the nanofilms was measured by atomic force microscopy (AFM, Dimension ICON). The contact angle of the nanofilms was measured using a contact angle meter (OCA20, Dataphysics). XRD analysis was performed using a Cu  $K\alpha$  irradiation source ( $\lambda = 1.5418 \text{ \AA}$ , Bruker D8 Discover) x-ray diffractometer. The sensing properties of the nanofilms were determined using a laboratory-made sensing platform.

### 1.3 Preparation of Analyte Vapors.

For vapor phase sensing of liquid analytes, the analyte to be tested (e.g., DCP) is prepared as follows: 50 mL of liquid DCP is placed in a 500 mL brown bottle, sealed, and kept under test conditions for 24 hours. This allows the system to reach gas-liquid equilibrium, resulting in the gas inside the bottle being the saturated vapor of DCP. To obtain different concentrations of DCP vapor, the saturated vapor can be mixed with dry air using a syringe. The resulting mixture is then injected into a gas bag for subsequent testing.

## 1.4 Vapor phase sensing studies

The nanofilms were placed on a custom-built sensing platform in the lab for sensing characterization. An automatic air intake system was controlled by an electronic valve, with an air intake time of 3 seconds. Each sample was tested more than 5 times to ensure the accuracy of the experimental data. The response of the films to DCP vapors was quantified by changes in fluorescence intensity ( $\Delta$ ). The relative change in fluorescence intensity is calculated using the following equation:

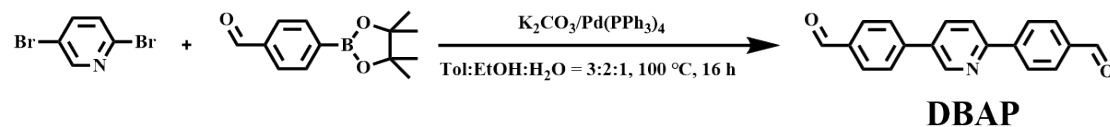
$$\Delta = \frac{I - I_0}{I_0} \times 100\%$$

where  $I$  is the fluorescence intensity at some point after analyte entry, and  $I_0$  is the fluorescence intensity in the initial state. It is worth stating, the concentration of the injected vapor can be calculated by the following equation,

$$C_A(\text{ppm}) = \frac{P_A}{P_{am}} \times 10^6$$

where  $P_A$  is the saturated vapor pressure of the liquid analyte at the test temperature,  $P_{am}$  is the atmospheric pressure at the test temperature.

## 1.5 Synthetic route to the compound DBAP



1,4-Dibromobenzene (236.9 mg, 1.0 mmol, 1.0 eq.),  $K_2CO_3$  (552.9 mg, 4.0 mmol, 4.0 eq.), and 4-Aminophenylboronic acid pinacol ester were dissolved in toluene (18 mL), ethanol (12 mL), and water (6 mL). The flask was charged with argon and tetrakis(triphenylphosphine)palladium (115.6 mg, 0.1 mmol, 0.1 eq.) was added. The reaction was heated to 95 °C and stirred for 16 h. The reaction was stopped and extracted with ethyl acetate. The obtained aqueous phase was extracted three times with ethyl acetate, the organic phase was mixed and washed with saturated brine and dried over anhydrous sodium sulfate. After extraction and spin-drying the product was purified by column chromatography, the eluent used was pure dichloromethane. DBAP (149 mg, 0.52 mmol, 52%) was obtained as a white solid.  $^1H$  NMR (600 MHz, Chloroform- $d$ )  $\delta$  10.10 (d,  $J = 3.2$  Hz, 2H), 9.03 (d,  $J = 2.3$  Hz, 1H), 8.26 (d,  $J = 8.0$  Hz, 2H), 8.08 (d,  $J = 10.6$  Hz, 1H), 8.03 (d,  $J = 5.9$  Hz, 4H), 7.95 (d,  $J = 8.2$  Hz, 1H),

7.83 (d,  $J = 7.9$  Hz, 2H). HRMS (APCI)  $m/z$ : calcd. for  $[M+H]^+$   $C_{19}H_{13}NO_2$ : 288.1019, found 288.1015.

### **1.6 Preparation of fluorescent nanofilm DBAP-ETTA**

The process of nanofilm DBAP-ETTA preparation was the same for different concentrations, and the detailed preparation conditions are shown in Table 1. As an example, the preparation steps for a nanofilm with a concentration of 0.5% (w%) are presented.

ETTA (0.81 mg, 2.06 mmol, 1.0 eq.) and DBAP (1.19 mg, 4.12 mmol, 2.0 eq.) were weighed and dissolved in 400  $\mu$ L of DMSO to form the precursor solution. After sonication to ensure complete dissolution, 100  $\mu$ L of the solution was taken and added dropwise to a pre-cleaned glass plate (2 cm  $\times$  2 cm), which had been cleaned using a mixture of  $H_2SO_4$  and  $H_2O_2$ . The glass plate was then placed in a constant temperature and humidity chamber set to 25  $^{\circ}C$  and 60% humidity. After 6 hours, the glass plate was removed and placed on the surface of water, allowing the nanofilm to separate and float on the water surface. After thorough cleaning, the nanofilm can be transferred onto various substrate surfaces such as quartz wafers, silicon wafers, etc., for different applications.

### **1.7 Preparation of control nanofilm TPDA -ETTA**

The nanofilm TPDA-ETTA was prepared by reacting ETTA (0.81 mg, 2.06 mmol, 1.0 eq.) with TPDA (1.19 mg, 4.12 mmol, 2.0 eq.) in 400  $\mu$ L of DMSO. The preparation procedure for TPDA-ETTA was similar to that of the DBAP-ETTA nanofilm.

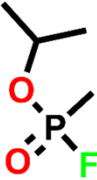
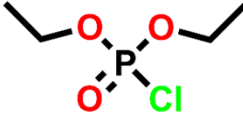
### **1.8 Sensing test conditions**

Temperature: 24 - 25 $^{\circ}C$ , consistently maintained throughout the experiment.  
Humidity: ranging from 54% to 56%.

## 2. Supplementary Table and Figures

**Table 1** Preparation conditions for nanofilms at different concentrations, with a molar ratio = 2:1 for DBAP/ETTA.

Entry	Concentration (wt%)	Temperature (°C)	Humidity (%)	Time (h)	Morphology	Solvent	Area (cm <sup>2</sup> )
1	0.25	25	60	8	Smooth		
2	0.5	25	60	6	Smooth		
3	0.75	25	60	6	Smooth	DMSO	4
4	1	25	60	6	Smooth		
5	0.5	30	60	5.5	Smooth		
6	0.5	35	50	6	Smooth		

Structure of Sarin	Structure of DCP
	

**Scheme S1.** Structure of sarin with diethyl chlorophosphate (DCP).

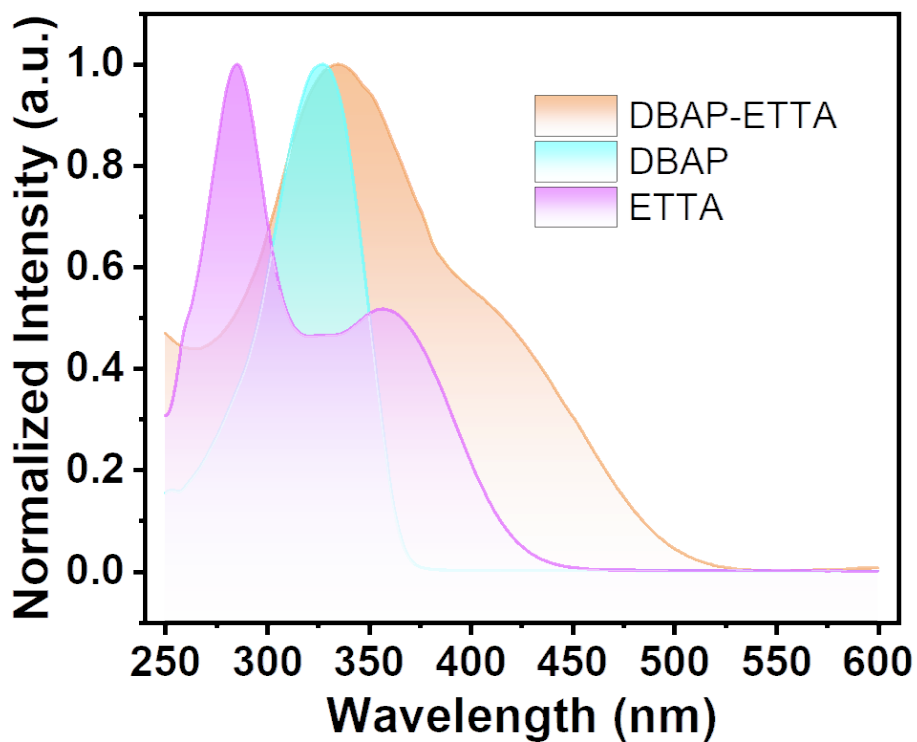


**Figure S1.** Absorption spectra of the compounds DBAP, ETTA, and DBAP-ETTA.

*Note:* The monomers DBAP and ETTA are in DMSO solution with a concentration of  $1 \times 10^{-5}$  mol/L, while DBAP-ETTA is in the film state.

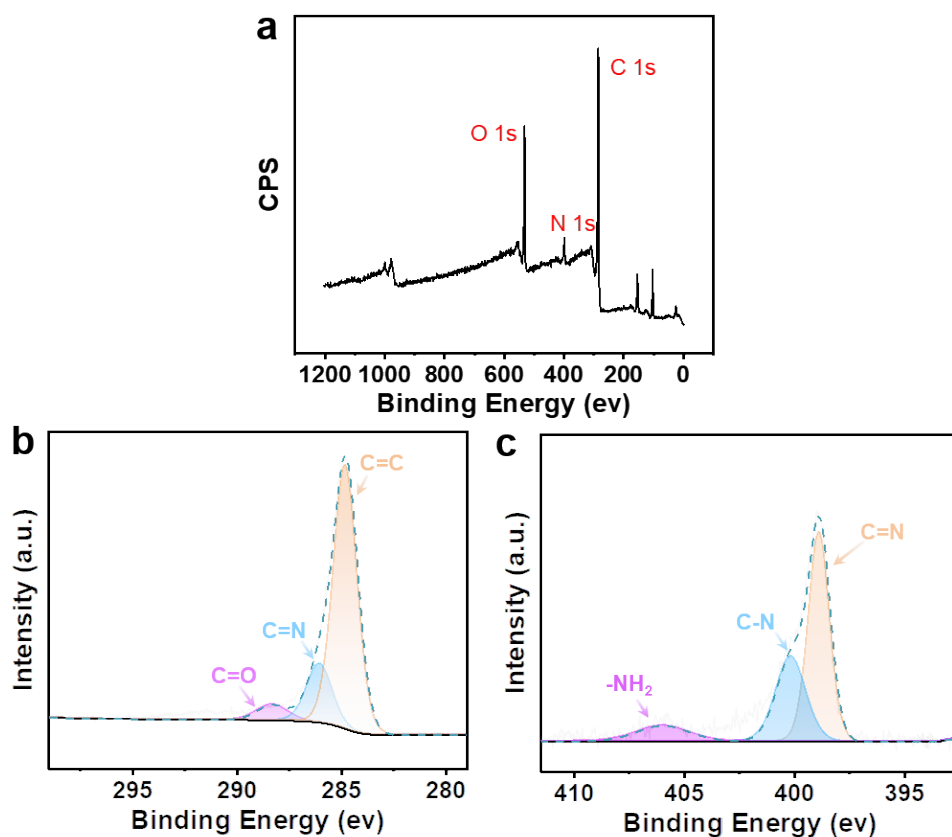


**Figure S2.** (a) XPS spectra of the nanofilm DBAP-ETTA. (b) C 1s XPS spectrum of DBAP-ETTA. (c) N 1s XPS spectrum of DBAP-ETTA.

*Note:* -NH<sub>2</sub> and -CHO peaks originate from a small amount of unreacted monomer.



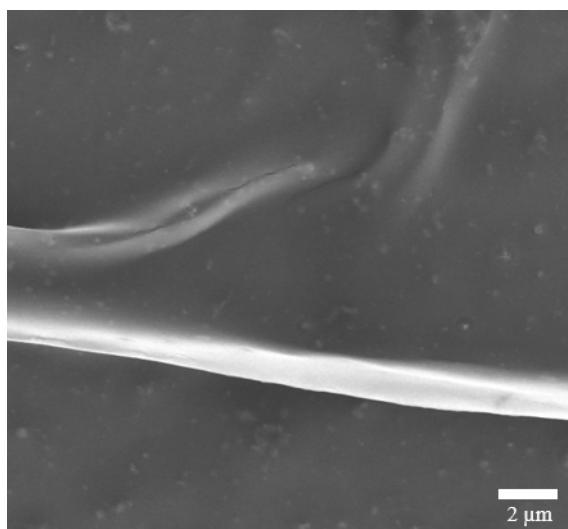


**Figure S3.** SEM images of nanofilm folds, demonstrating the film's good flexibility at a microscopic level.

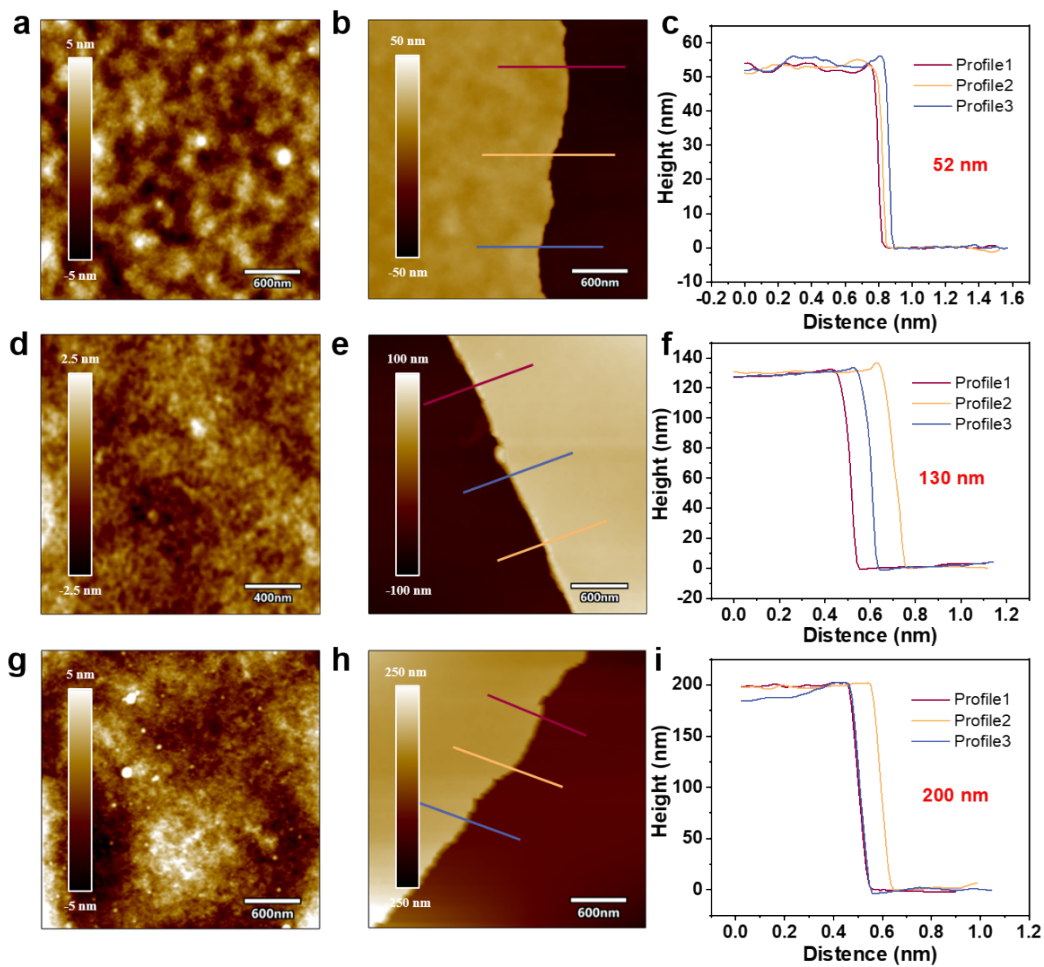


**Figure S4.** Thickness and surface morphology of nanofilms prepared with different concentrations of precursor solutions. (a-c) w% = 0.25%. (d-f) w% = 0.75%. (g-i) w% = 1.00%.

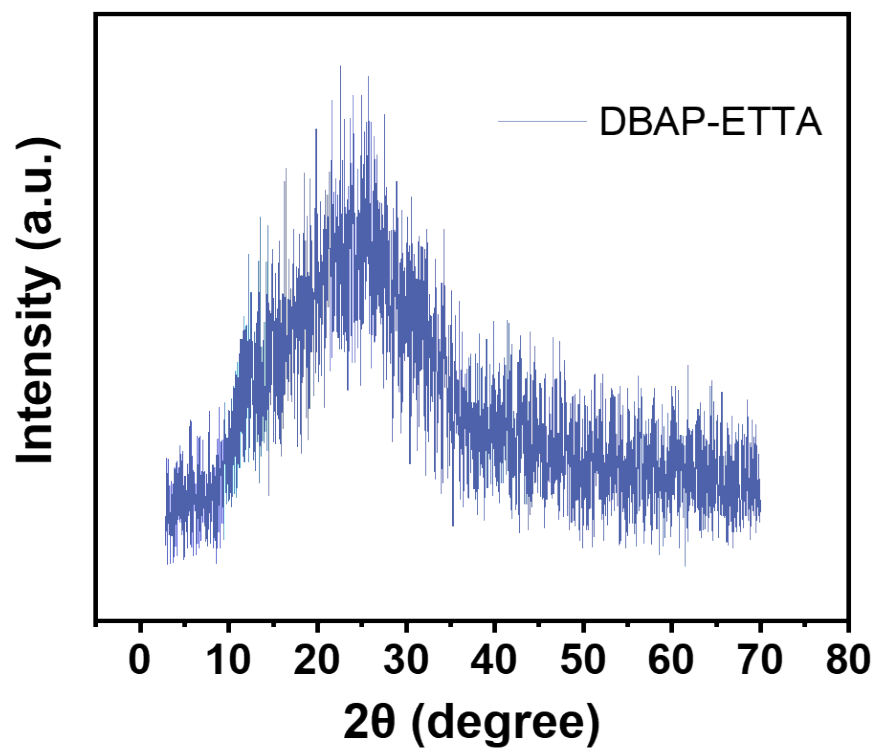


**Figure S5.** Powder XRD of the nanofilm DBAP-ETTA.

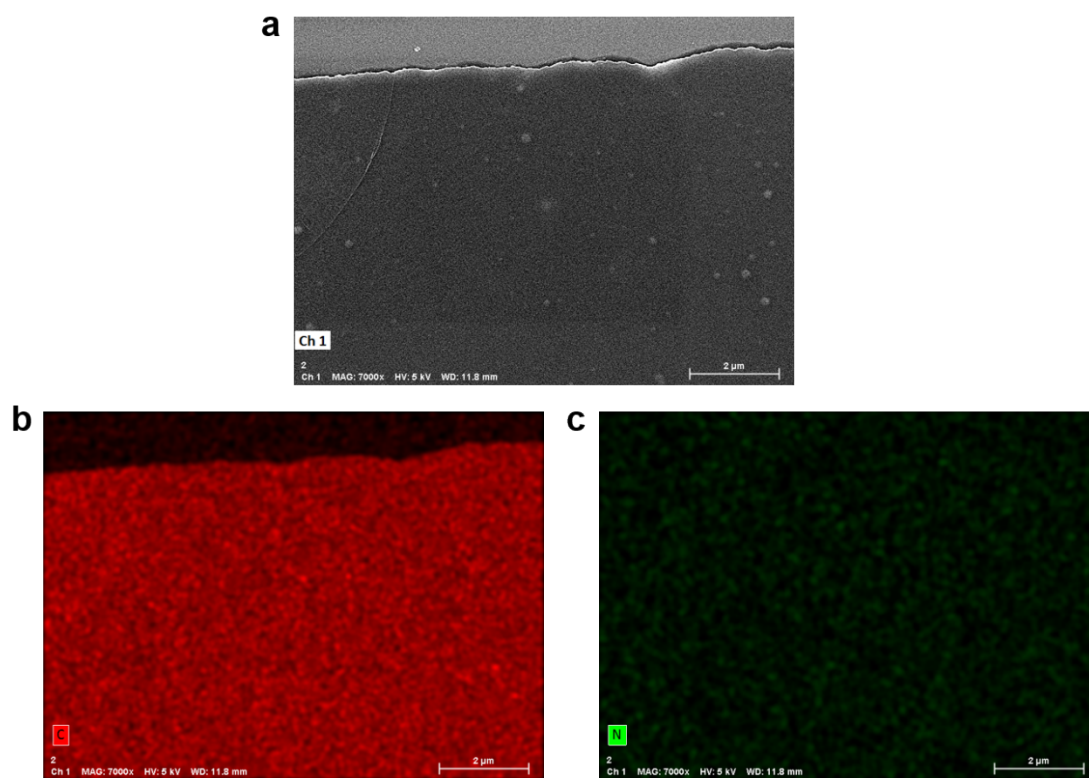
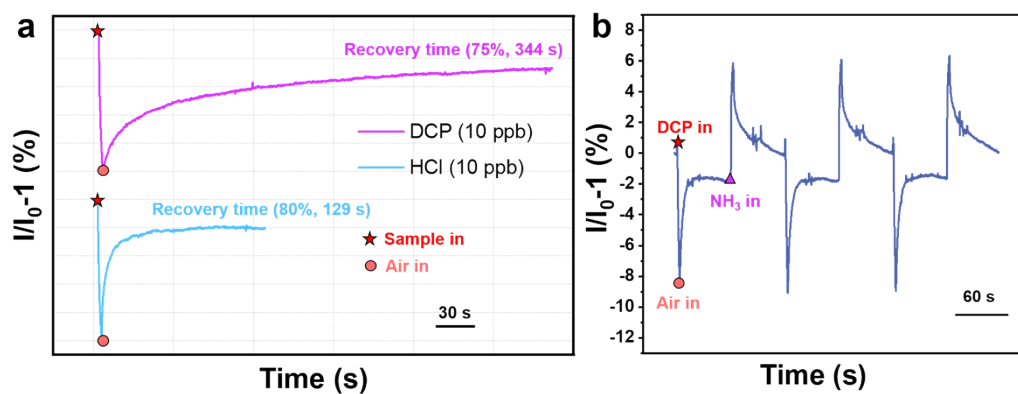


**Figure S6.** EDX element mapping of DBAP-ETTA. (a) Morphology of nanofilm DBAP-ETTA. (b) Area distribution of element C. (c) Area distribution of element N.



**Fig**

**ure S7.** (a) Response kinetics curve of DBAP-ETTA to DCP vapor (10 ppb) and hydrochloric acid vapor (10 ppb). (b) Detailed response curves for partial spontaneous recovery after air purge and full recovery after  $\text{NH}_3$  treatment.

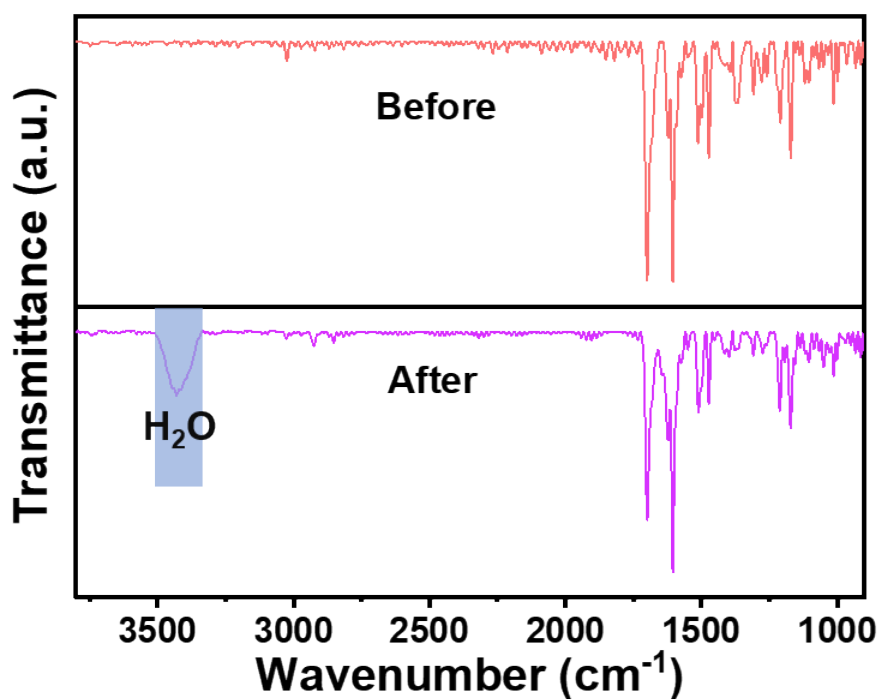


**Figure S8** FT-IR spectra of the nanofilm DBAP-ETTA before and after DCP treatment.

*Note:* The red line shows the FT-IR spectra of the initial nanofilm before DCP treatment. The measurement was carried out after the sample were dried overnight in an oven.

While the purple line is the FT-IR spectra of the nanofilm after DCP treatment. The water is necessary for the DCP hydrolysis process, thus the humidity was maintained ranging from 54% to 56% during the sensing tests. And the sample was measured immediately after DCP vapor fumigation without additional drying. Therefore, there's a water peak in the purple line at 3440 cm<sup>-1</sup>.

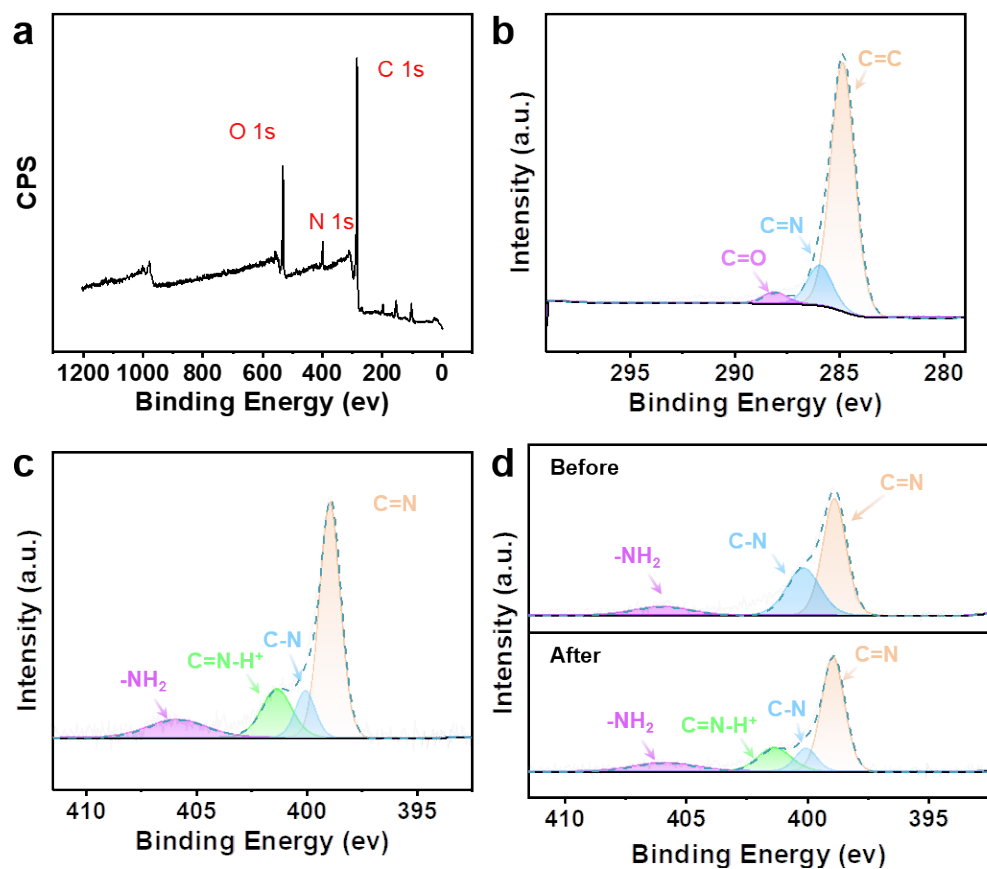


**Figure S9.** (a) XPS spectra of the nanofilm DBAP-ETTA after DCP treatment. (b) C 1s XPS spectrum of DBAP-ETTA after DCP treatment. (c) N 1s XPS spectrum of DBAP-ETTA after DCP treatment. (d) N 1s XPS spectrum of DBAP-ETTA before and after DCP treatment.

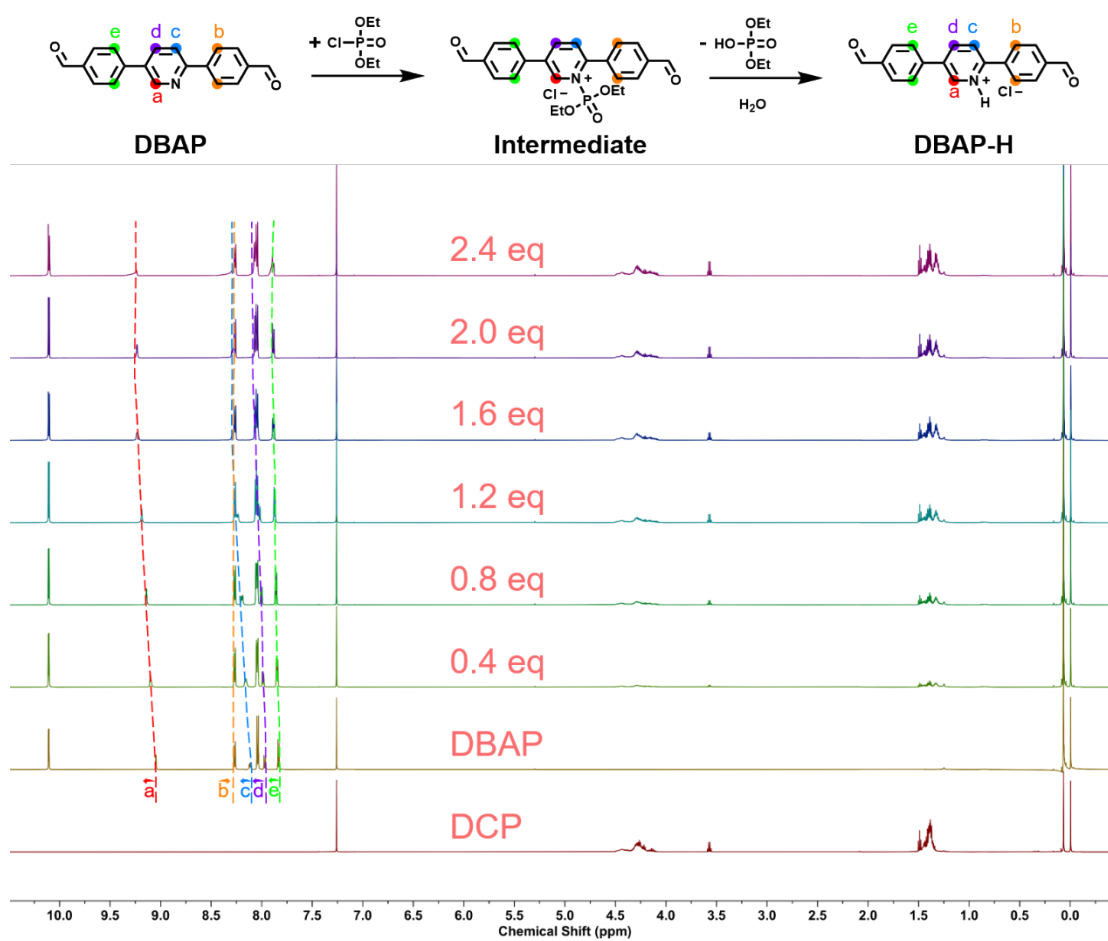


**Figure S10**  $^1\text{H NMR}$  spectra of the compound DBAP with different equivalence ratios of DCP addition (600 MHz,  $\text{CDCl}_3$ ).



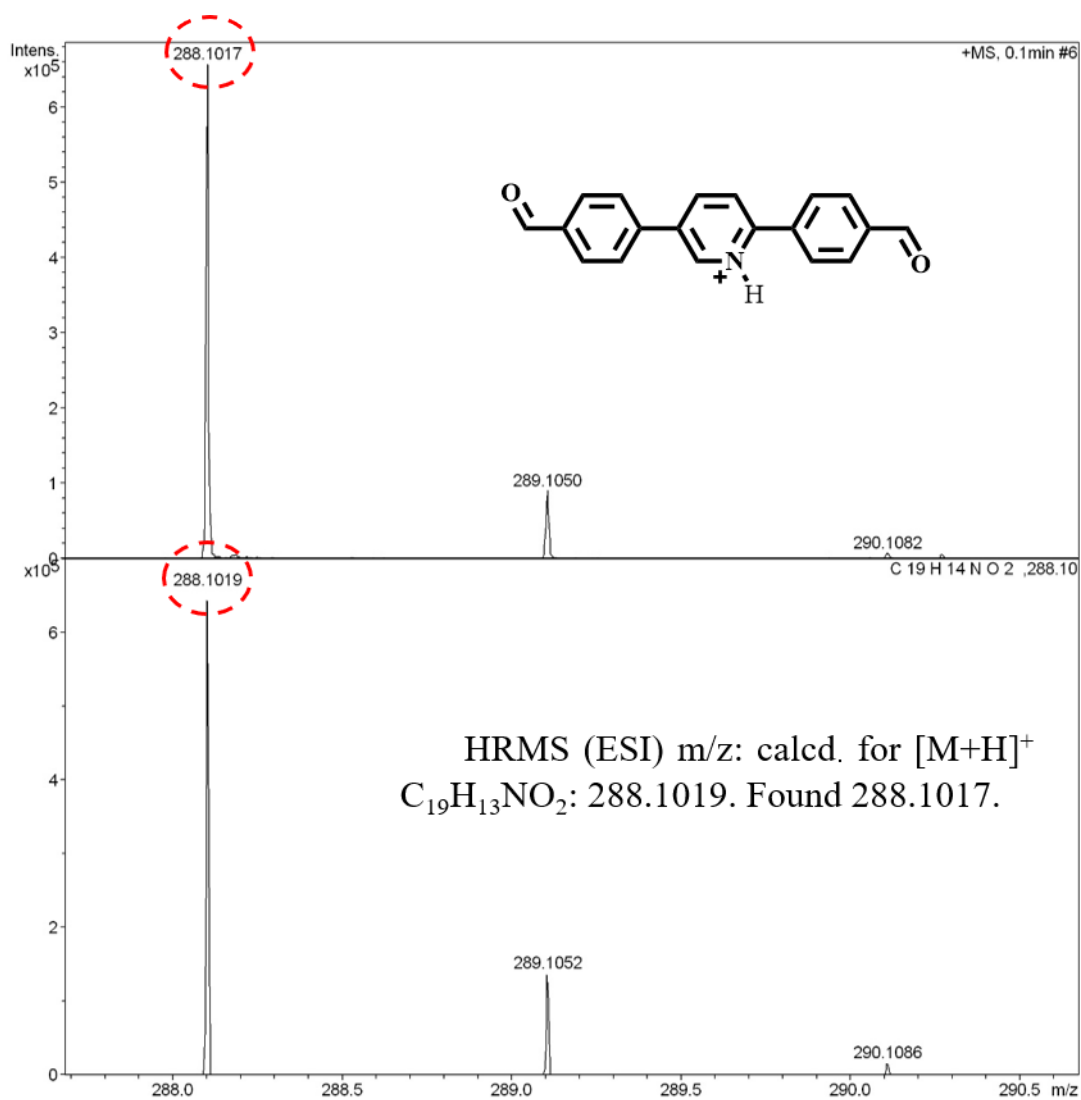


**Figure S11.** HRMS spectrum of DBAP-H.

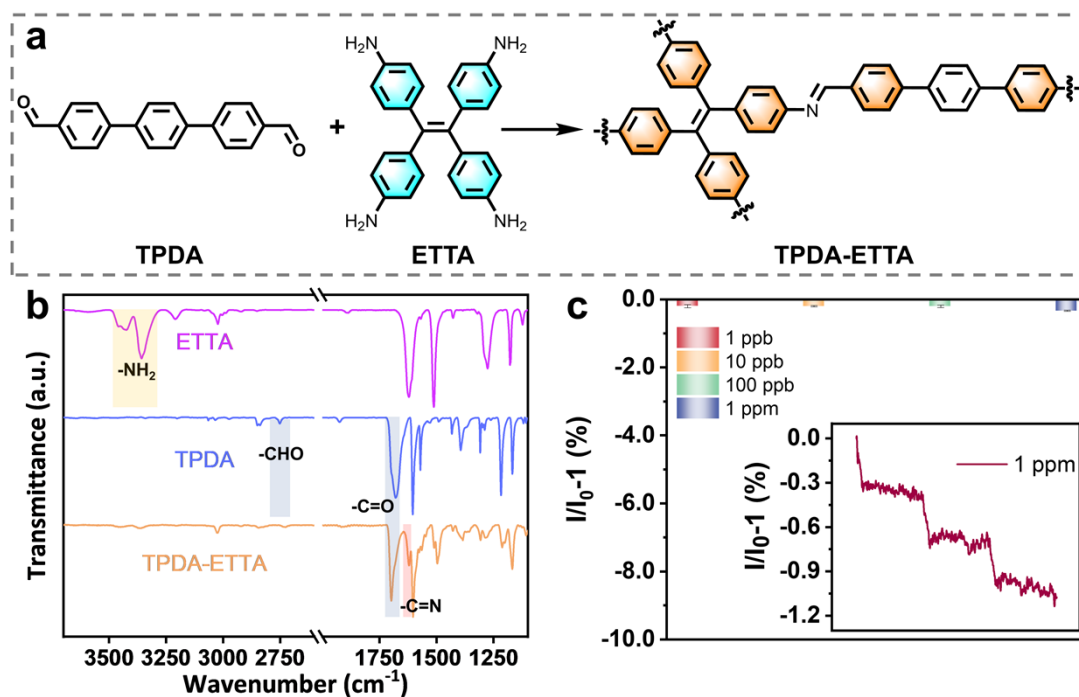


**Figure S12.** (a) Structure of nanofilm TPDA-ETTA. (b) FT-IR spectra of ETTA, TPDA and the nanofilm TPDA-ETTA. (c) Sensitivity test of nanofilm TPDA-ETTA, inset shows the response curve of TPDA-ETTA to 1 ppm concentration of DCP vapor.

*Note:* As shown in Fig. S12, the nanofilm exhibits poor response strength (0.3%) to 1 ppm DCP vapors, and irreversible signals.

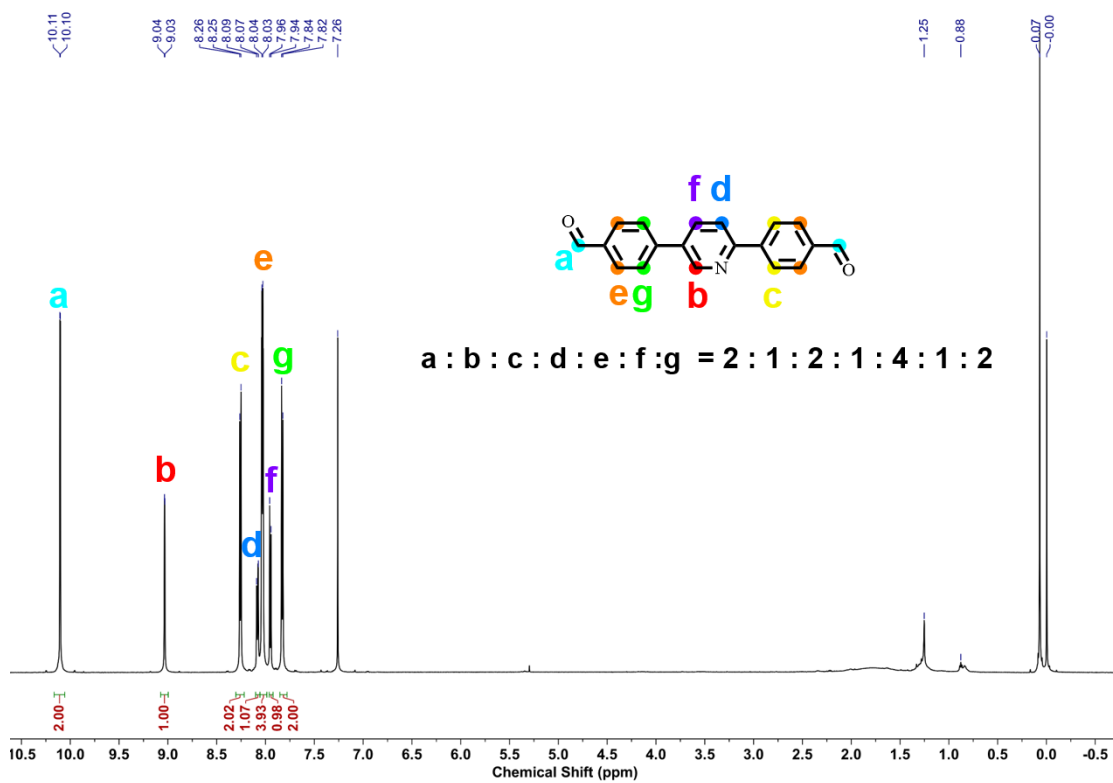


**Figure S13.**  $^1\text{H}$  NMR spectrum of DBAP (600 MHz,  $\text{CDCl}_3$ ).

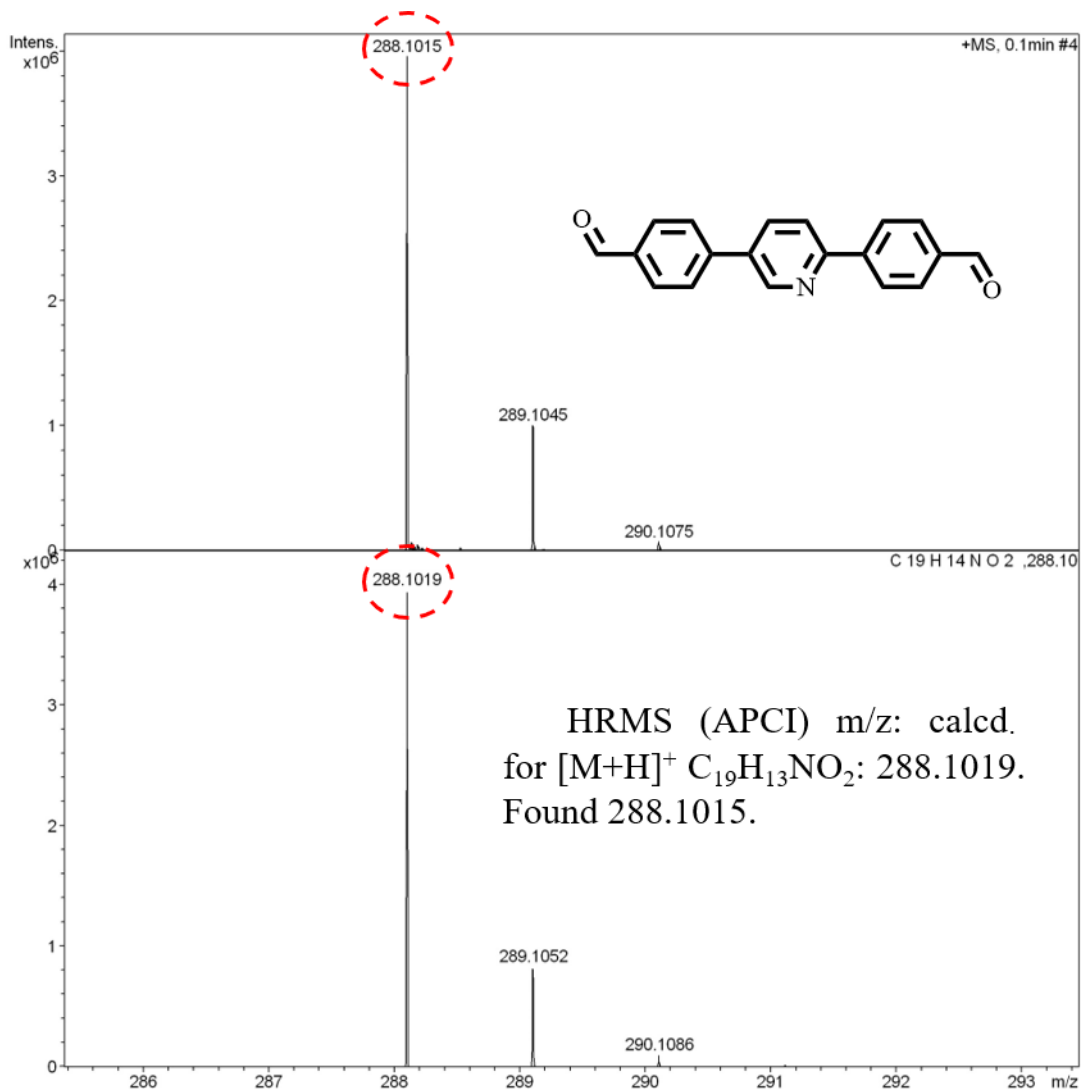


**Figure S14.** HRMS spectrum of DBAP.